Cite this article
Morley DG, Madabhushi GSP, Sakufiwa D and Thusyanthan I (2025)
Investigation into soil ratcheting behind integral bridges using centrifuge modelling.
Proceedings of the Institution of Civil Engineers – Bridge Engineering **178(4)**: 373–389,
https://doi.org/10.1680/jbren.23.00046

Research Article
Paper 2300046
Received 10/11/2023;
Accepted 12/03/2024

Bridge Engineering

Investigation into soil ratcheting behind integral bridges using centrifuge modelling

Douglas G. Morley MEng, MRes
PhD student, Department of Engineering, University of Cambridge, Cambridge, UK (Orcid:0000-0001-8320-1841) (corresponding author: dm909@cam.ac.uk)

Gopal S.P. Madabhushi PhD, FICE
Professor, Department of Engineering, University of Cambridge, Cambridge, UK (Orcid:0000-0003-4031-8761)

Dennis Sakufiwa CEng, MICE
Head of Geotechnics, National Highways, Leeds, UK

Indrasenan Thusyanthan MEng, PhD (Cantab), FICE, CEng, CMarEng
Global Offshore Director, Gavin & Doherty Geosolutions (GDG) Ltd, Dublin, Ireland (Orcid:0000-0001-8196-4335)

Integral bridges in the UK are commonly designed according to PD 6694-1:2011, with guidance on backfill ratcheting based on experimental data that is limited by testing at a small-scale low-stress state, a lack of abutment foundation and soil below, and a limited range of soil–structure configurations. As integral bridge use increases, there is a need for further understanding of the strain ratcheting mechanism, which can lead to smarter designs that minimise material usage and lifetime maintenance. The suitability of modern centrifuge techniques to simulate ratcheting of soil behind an integral bridge abutment over a design life of thermal loading was investigated. A high-accuracy actuation system was developed and employed in centrifuge testing, with test data provided to demonstrate its capabilities. Surface settlements, deck axial forces and abutment bending moment distributions recorded for various soil–structure combinations were compared, highlighting the sensitivity of soil ratcheting. This work shows that centrifuge modelling can successfully simulate backfill strain ratcheting behind integral abutments over a range of soil–structure configurations. Furthermore, the results suggest that global rotations and base sliding are significant to the overall response, clarifying the importance of modelling at an appropriate stress state with a foundation and the soil below.

Keywords: bridges/centrifuge modelling/temperature-related & thermal effects/soil–structure interaction

1. Introduction

Integral bridges have become a first-choice typology in the UK and USA due to their low maintenance needs, attributed to the absence of bearings and expansion joints, as depicted in Figure 1. However, the removal of these structural components introduces a level of uncertainty in bridge analysis and design, largely stemming from thermal movements of the long deck members that interact with the backfill soil retained by the abutments. This thermal movement gives rise to various challenges, notably thermal stresses due to the restraint of large structural members without any joints and variable soil stresses in the backfill acting on the abutments. This issue of soil–structure interaction is twofold. During high-temperature periods, expansion of the bridge deck forces the abutments into the backfill, mobilising high earth pressures and hence large abutment bending moments. Conversely, in colder temperatures, the abutments pull away from the backfill, permitting the retained soil to settle at the bridge approach. These two phenomena have a cyclic dependence and worsen with time. The first of these is known as 'strain ratcheting'.

The so-called strain ratcheting of earth pressures behind integral abutments is a complex mechanism influenced by various geotechnical and structural variables, making it a challenge to characterise in design codes. Collection of data is required to better understand the process. However, instrumenting and monitoring full-scale structures is costly and time intensive, while small-scale modelling is carried out at an inappropriate soil stress state and is hence limited to finding trends. Furthermore, finite-element models are unable to simulate particle rearrangement in the backfill without careful calibration.

Geotechnical centrifuge modelling is an alternative that can replicate the true earth pressures behind full-size integral abutments, while being cost and time effective. It therefore provides an efficient means for testing a range of soil–structure configurations to inform the next revision of design codes. This work presents the methodology and preliminary results of a centrifuge modelling campaign, showing how parametric studies can help to increase the use and structural efficiency of integral bridges, for greater resilience across infrastructure networks.

2. Background

Integral bridges have been a part of the UK's structural landscape since the 1950s, although the jointless typology dates back much further, in the form of masonry arch structures (Hambly, 1997). Integral bridges have been used more extensively in the USA, with over 9000 built nationwide (White, 2007). This typology is unproblematic until span lengths and skews are increased, at which point temperature-induced movements become a concern.

Many of the uncertainties associated with integral bridge design arise from soil–structure interaction, as thermal movements of the deck repeatedly thrust the abutments into and away from the retained backfill, as shown in Figure 2. Strains imposed on the soil by the abutments lead to stress transfer back onto the structure, increasing the bending moments and axial force within the bridge deck. An increase in lateral pressures over thermal cycles due to strain accumulation – known as strain ratcheting – is a complex mechanism, seemingly fuelled by the settlement of soil during deck contraction phases. Understanding and predicting the extent of strain ratcheting is a challenge since it is influenced by a variety of geotechnical and structural parameters, including the soil friction angle, uniformity coefficient, particle size and angularity, soil–structure relative stiffness, soil–structure interface friction and foundation type. The earth pressures generated reflect the straining imposed from the deflected shape of the abutment, which in turn is dependent upon the earth pressures imposed. Therefore, efficient integral abutment design requires an iterative approach (Wiechecki *et al.*, 2023).

2.1 Design code development

In the late 1990s and early 2000s, the UK Transport Research Laboratory (TRL) produced several reports exploring various aspects of integral bridge behaviour. Research included assessing the performance of existing bridges (Barker and Carder, 2000, 2001; Darley *et al.*, 1996, 1998; Darley and Alderman, 1995), investigating compressible materials as a means to accommodate

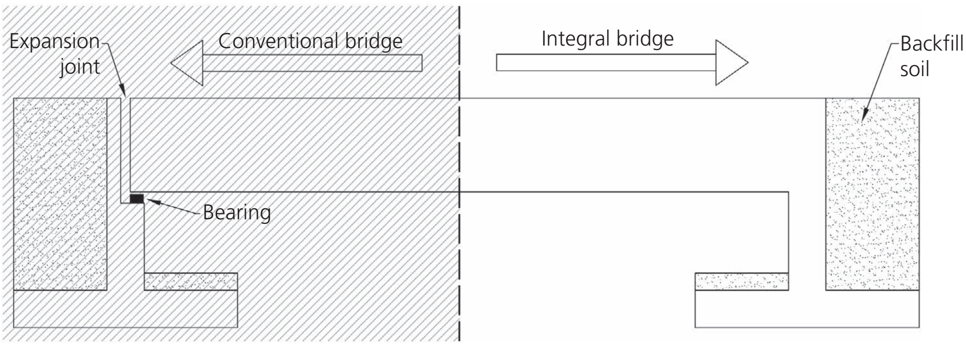

Figure 1. Integral bridge typology

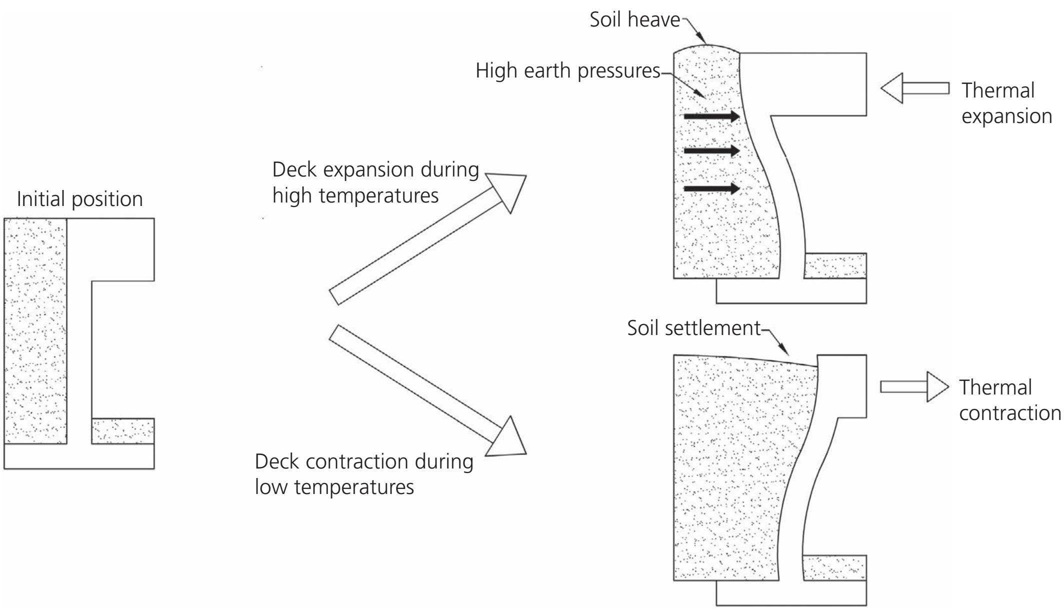

Figure 2. Soil–structure interaction due to thermal effects on bridge deck

thermal movements (Carder *et al.*, 2002a, 2002b; Carder and Card, 1997; Darley and Carder, 1998) and a centrifuge modelling campaign to examine the performance of an integral bridge with two foundation types (Springman *et al.*, 1996). Several of these reports were referenced by the now-superseded design guidance in BA 42/96 of the *Design Manual for Roads and Bridges* (DMRB) (HA, 2003). Combining this research with testing conducted by England *et al.* (2000), BA 42/96 relied on data from a combination of full-scale monitoring, centrifuge modelling and small-scale tests. Along with several other DMRB documents, BA 42/96 was replaced by PD 6694-1:2011 (BSI, 2020) in 2011. Section 9 of PD 6694-1:2011 (covering integral bridges) shares many similarities with BA 42/96, but incorporates findings from two additional centrifuge tests (Tan and Lehane, 2007; Tapper and Lehane, 2004) and material testing conducted by Clayton *et al.* (2006). The work of Denton *et al.* (2011) explains some of the changes made in this transition, and makes clear the influence of the small-scale testing conducted by England *et al.* (2000).

PD 6694-1:2011 (BSI, 2020) cites four physical modelling campaigns, with three of these conducted in a geotechnical centrifuge at enhanced accelerations. The other work, carried out by England *et al.* (2000) for the Highways Agency, used a small-scale testing setup that applied horizontal displacement cycles to a 520 mm rigid wall with a pinned base and retaining backfill soil. As a small-scale experiment, it was limited by the soil existing at a lower stress state than that behind a full-size bridge. The soil would therefore have behaved with an increased stiffness and experienced excessive dilation (and hence surface heave) due to reduced confinement (Madabhushi, 2014). Additionally, the abutment was modelled without a footing or foundation soil; while this would have helped isolate the ratcheting mechanism, it would also have altered the abutment deflection and so imposed soil straining, as well as prevented the influence of global mechanisms such as abutment translation and rotation. The experiments conducted by Tapper and Lehane (2004) and Tan and Lehane (2007) were similar to those carried out by England *et al.* (2000), except they were conducted in a high-gravity environment to replicate the soil stress distribution of a full-size integral bridge. The last of the four tests referenced by PD 6694-1:2011 – a TRL document authored by Springman *et al.* (1996) – reported the testing of two integral abutments with realistic boundary conditions. This work presented the results of nine centrifuge tests on both an embedded wall and a spread-based abutment foundation, with parameters such as sand density and abutment stiffness being altered.

Uncertainty in the strain ratcheting of backfill behind integral bridges led to the former code BA 42/96 (HA, 2003) setting a span length of 60 m on its requirement for all bridges to be integral where possible. Furthermore, doubt was also reflected in the scope being limited to bridges with thermal movements not exceeding ±20 mm at each abutment and skews no higher than 30°. The limit equilibrium method (LEM) in the current guidance PD 6694-1:2011 (BSI, 2020) does not make reference to a 60 m span length, but does adopt the same scope restrictions, with the thermal movement limit reworded to a 40 mm movement at the end of the deck. These limits are stringent compared with those in other countries, especially the USA (Abdel-Fattah *et al.*, 2018). A movement of 40 mm at the end of a concrete deck equates roughly to a 75 m span from the centre of the bridge (where the expansion is zero), giving a 150 m bridge length in total, or around 100 m if using a steel box section that has a higher temperature variation (Card and Carder, 1993). This is far beyond the spans typically used for integral bridges in the UK. Furthermore, field monitoring reported by Skorpen *et al.* (2020) suggests that thermal movements can be much smaller than those predicted due to the thermal inertia of the bridge deck.

2.2 Construction techniques

Several strategies have emerged to eliminate some of the uncertainty that exists in the design of integral bridges. Run-on slabs are not uncommon in bridges globally and, behind integral bridges where large settlements are known to occur, they are widely used (White, 2007) and supported by research (Springman *et al.*, 1996). However, the UK's PD 6694-1:2011 (BSI, 2020) is one of the few codes that does not recommend them. Work by Cosgrove and Lehane (2003) and Tapper and Lehane (2004) provides insights into recommended slab lengths for various foundation types.

To deal with the stress increase associated with soil strain ratcheting, a growing trend in the UK and Sweden involves casting abutment columns within sleeves in a self-supporting reinforced soil wall (RSW) to allow free movement. While used, seemingly successfully, to mitigate the soil–structure interaction, this approach requires the abutment to be set back behind the face of the RSW, increasing span length, and may lead to a thicker abutment since it is no longer restrained against buckling (White, 2007). Also, controls are required to ensure the gap between the abutment columns and sleeves remains functional in the long term. A thoughtful approach – and one that has been considered for a long time – is the use of a compressible material between the abutments and backfill that can accommodate thermal movements and minimise soil disturbance. Reports published by the TRL discuss a range of materials suitable for this purpose, most notably expanded polystyrene (EPS) geofoam, along with essential material requirements such as the elastic range, stiffness and strength (Carder *et al.*, 2002a, 2002b; Carder and Card, 1997; Darley and Carder, 1998). Numerical work by Caristo *et al.* (2018) found a seven times reduction in peak earth pressure when using rubber to isolate the backfill. There is, however, a need to investigate compressible inclusions experimentally in order to complement the numerical work carried out and to confirm whether there is merit in their use.

2.3 Further research

Research is required to gain a deeper insight into the parameters that influence integral bridge behaviour. Work by Sandberg *et al.* (2020) and Morley *et al.* (2024) suggests that altering the relative stiffness of the soil and structure could significantly enhance bridge response through an altered abutment deflected shape, and hence soil straining. This idea is supported by Wood (2004), who also challenged the significance of the friction angle in backfill ratcheting, in contrast to the guidance given in PD 6694-1:2011 (BSI, 2020) regarding backfill soil type. By investigating the influence of parameters through physical and numerical modelling, the equation in the LEM of PD 6694-1:2011 (BSI, 2020) for the design value of the earth pressure coefficient for expansion, K_d^*, can be improved. Some key parameters include the relative soil–structure stiffness, the foundation type, backfill soil type and founding soil strength.

The USA, among other countries, has a long history of building large-span integral bridges (Hambly, 1997), which the UK does not. To this end, it is interesting to consider the practical approach to research taken in South Africa, where a full-scale 90 m integral bridge was constructed and extensively instrumented (Skorpen *et al.*, 2018, 2020). The data showed considerably less ratcheting than expected, hence setting the precedent for the use of larger spans in this climate. It also questions the reliance of PD 6694-1:2011 (BSI, 2020) on modelling data, which may exaggerate ratcheting through a misrepresentation of field conditions such as the magnitude of thermal movements and moisture content of the backfill.

3. Centrifuge modelling of integral bridge abutments

3.1 Centrifuge modelling

Geotechnical centrifuge modelling has a history spanning over half a century, as discussed by Schofield (1980). Using either a so-called drum or beam centrifuge, a small-scale model is spun at a high angular velocity, generating a centrifugal force that enhances the vertical accelerations or 'gravity' acting on the model. This has the effect of augmenting the body weight of each soil particle and consequently the stress distribution with depth. This process therefore replicates the stress–strain conditions found in a much larger soil continuum, and can be used to create parity between a small-scale model and a full-size geotechnical problem. Despite this realism, decisions are often made to isolate variables and underlying mechanisms rather than setting conditions true to the complex field structure, as is the case with most modelling. Centrifuge scaling laws have been established to transition between scales, some of which are shown in Table 1.

Table 1. Centrifuge scaling laws (Madabhushi, 2014)

	Scaling law (model : full-size)
Gravity	$N:1$
Length/displacement	$1:N$
Stress	1 : 1
Strain	1 : 1
Force	$1:N^2$
Flexural stiffness (EI/m)	$1:N^3$
Bending moment (Nm/m)	$1:N^2$

Geotechnical centrifuge modelling shares the advantages of small-scale modelling (the quick and cost-effective preparation of models), but can go further by recreating the stress–strain conditions of a full-size geotechnical problem. Therefore, the mechanisms and magnitudes of findings can be relied upon to give indications for real-world field scenarios. The challenges of centrifuge modelling are predominantly in getting access to a centrifuge and the requisite modelling expertise. Kim *et al.* (2013) reported that, at the time of writing, there were over 110 geotechnical centrifuges in operation globally. The majority of these were based at academic institutions engaging in collaborative projects with industry; in some regions, contractors have their own centrifuges and integrate results into project tenders.

The Schofield Centre at the University of Cambridge has both a drum and beam centrifuge. The 10 m dia. Turner beam centrifuge, shown in Figure 3, became operational in the late 1970s (Madabhushi, 2014; Schofield, 1980). It is a 150 ***g***.t machine, meaning it can subject a 1 t model to an enhanced vertical acceleration of 150 times Earth's gravity (***g***). With this capacity it becomes possible to model a wide range of geotechnical scenarios, including those involving tunnels, wind turbine foundations and retaining walls. A challenge in modelling soil–structure interaction scenarios such as these is the design of equipment that functions under enhanced gravity conditions.

3.2 Integral bridge model

A model was designed for testing in the Turner beam centrifuge, as shown in Figure 4. The model's dimensions were selected based on an array of sources, including constructed bridges, physical models and numerical models to represent typical characteristics of an integral bridge (Argyroudis *et al.*, 2016; Barker and Carder, 2001; Carder, 1998; Craig and Knappett, 2020; Darley and Alderman, 1995; Khodair and Hassiotis, 2005; Kolay *et al.*, 2013; Lancellotta, 2009; Lehane *et al.*, 1999; Ng *et al.*, 1998; Trenter, 2004). A 9 m abutment and 6 m spread footing were taken to represent something at the larger end of conventional design. A spread footing was chosen over a single row of piles to meet the conditions of the LEM in PD 6694-1:2011 (BSI, 2020), as well as to aid in the

Figure 3. Turner beam centrifuge (10 m in diameter) at the Schofield Centre, University of Cambridge

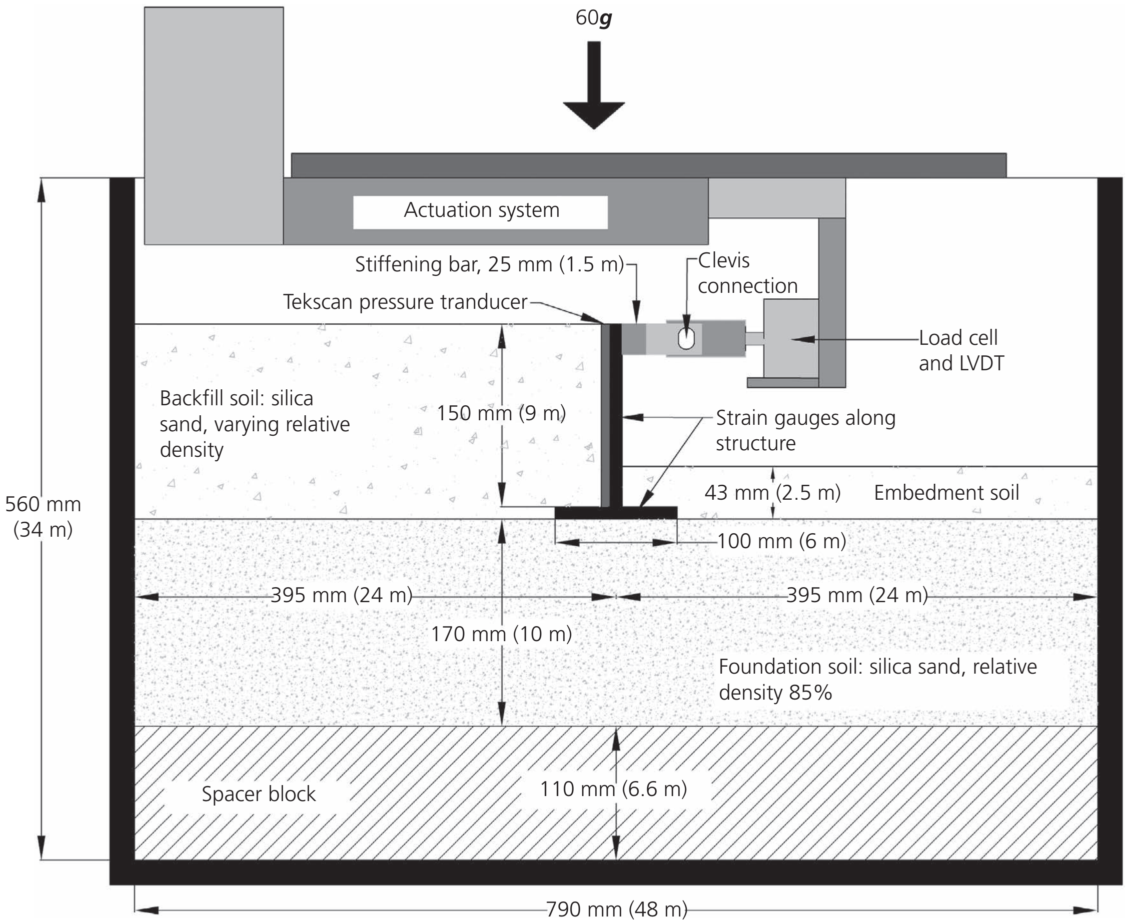

Figure 4. Schematic diagram of integral bridge centrifuge model

interpretation of data by assuming plane strain conditions and observing foundation movements during testing. Symmetry of the problem allowed for the modelling of only half the bridge.

Thermal cycles were applied through a mechanical actuator able to provide force or displacement control for any number of cycles at a programmable rate and magnitude, making it more versatile than applying heating and cooling directly. The bridge deck was omitted from the model and hence the actuator was connected to the abutment by way of a pin and clevis connection, preventing moment transfer. The connection was made by a stiffening bar, scaled based on a 1.5 m thick equivalent bridge deck. While real abutments are unlikely to undergo the degree of top rotation permitted with this pinned connection, it provided a known boundary condition and also allowed for accurate control of the actuator, therefore making a robust examination of the ratcheting phenomena possible. Testing by England *et al*. (2000), Tapper and Lehane (2004) and Tan and Lehane (2007), cited in PD 6694-1:2011, was carried out in a similar way. The impact on results was a lack of hogging moment transferred from the deck, as well as an altered joint rotation changing the deflected shape of the abutment. Future studies may look to relate findings to an abutment with a more realistic connection and try to model a contribution from the bridge deck, as attempted by Springman *et al*. (1996).

3.2.1 Model scaling

The dimensions of the model container were 790 × 560 × 200 mm, so an appropriate centrifugal acceleration was selected to scale down the full-size structure. A value of 60***g*** was chosen to accommodate the abutment within the box, while maintaining a sufficient distance between the footing and container base as well as between the abutment and container wall in order to prevent boundary effects. Furthermore, 60***g*** was the minimum value at which this could be achieved, therefore limiting errors associated with modelling (Madabhushi, 2014). The limiting lateral extent was determined by projecting a passive failure plane at the corner of the footing to the surface, based on Rankine's theory. The required depth of soil beneath the foundation was evaluated using the analytical Boussinesq solution. At this acceleration of 60***g***, an abutment width of 12 m could be modelled within the 200 mm box width, hence plane strain conditions were assumed with boundary effects at the centre of the box considered negligible.

3.2.2 Model abutment

Flexural stiffness is often the governing parameter when modelling retaining walls (Madabhushi, 2014) as it dictates the deflected shape of the structure and hence magnitude of soil straining. The scaling law presented in Table 1 was applied, transforming the 1 m cracked reinforced concrete (RC) reference structure (flexural stiffness (EI) of 2.1×10^6 kN.m^2/m) to aluminium of 12 mm thickness. A bolted connection was formed between the abutment and foundation. Alongside this reference structure, a more flexible 0.4 m abutment ($EI = 1.4 \times 10^5$ kN.m^2/m) and pinned foundation connection were modelled to assess their influence on ratcheting and structural response. The pinned connection was formed by joining the base of the abutment to the spread footing by way of a hinge, rather than bolts. Modelling with aluminium based on a cracked RC section was preferable as it eliminated the uncertainty of concrete cracking in a reduced-scale model section (and hence stiffness degradation) throughout testing, while still capturing the long-term behaviour. The downside was a reduced interface friction angle between the backfill and abutment.

3.2.3 Backfill and foundation soil

Hostun sand, with the properties detailed in Table 2, was used for testing. This sand has a smaller particle size than type 6N/P backfill typically used behind integral bridges. This is generally required in centrifuge modelling to ensure a sufficient number of particle–structure contacts, considering the scaled abutment dimensions (Madabhushi, 2014). Hostun sand is almost uniformly graded, with a friction angle at the low end of that expected for type 6N/P material, likely resulting in lower ratcheting pressures (BSI, 2020). In all tests, the founding soil was poured to attain a dense state, whereas the backfill was varied between dense (relative density (I_d) = 85%) and loose (I_d = 40%) in order to evaluate its effect on ratcheting behaviour. Air pluviation with an automatic sand pourer was used to achieve these void ratios consistently. The sand was dyed with black ink in a ratio of 1 : 3 so that particle movements could be tracked during testing.

3.2.4 Instrumentation

The model was instrumented to monitor both soil and structural behaviour during thermal cycles. A load cell and linear variable differential transformer (LVDT) were placed in alignment with the actuator–abutment connection to record abutment displacement and axial force within the bridge deck, while also allowing control over the actuator. A total of 12 full-bridge strain gauges were positioned along the abutment and footing to derive bending moments at roughly 1 m intervals (at full scale). A Tekscan tactile pressure transducer was placed between the abutment and backfill to gauge the magnitude and distribution of earth pressures along the abutment height. One wall of the strong box was made of Plexiglass to offer visibility into the model and allow for photos to be captured throughout the test. From these photos, GeoPIV-RG (Stanier *et al*., 2016; UWA and QUC, 2015) was used to track soil movement and abutment deflection over

Table 2. Hostun sand properties

Property	Value
Maximum void ratio	1.01
Minimum void ratio	0.555
Specific gravity	2.65
Median grain size	440 μm
Uniformity coefficient	1.67
Critical friction angle	33°

cycles using particle image velocimetry (PIV) techniques. This provided valuable insights into the ratcheting mechanism, surface soil settlement and the relationship between abutment deflection and earth pressure generation.

3.2.5 Actuation system

A mechanical actuator was developed to control the application of thermal cycles to the top of the abutment, in place of the bridge deck. The system was designed to adhere to the 40 mm movement limit prescribed by the LEM in PD 6694-1:2011 (BSI, 2020), equivalent to ±0.33 mm at the centrifuge scale. This represented a concrete bridge span of roughly 150 m. Meeting the sub-millimetre displacement requirement proved challenging due to elastic bending of the actuator frame. This was addressed by providing live control through a C++ script taking input from either the LVDT (for displacement control) or load cell (for force control) in-line with the actuator. Based on numerical modelling, a force of 4 kN at the centrifuge scale was deemed necessary to strain the soil by this amount (Morley *et al.*, 2022), although the actuator capacity was designed to provide 12 kN, giving the flexibility to test a range of abutment heights and cycle regimes.

3.3 Testing configurations

The final testing configuration is shown in Figure 5. Eight centrifuge tests were conducted over 2 years to examine the strain ratcheting behind integral bridges, as well as some parameters with bearing on the structural response. Six of these tests maintained a similar cycling regime while introducing variations to the soil–structure configuration, including changes to the abutment stiffness, abutment height, foundation–abutment connection, backfill density and the inclusion of geofoam. The remaining two tests explored the influence of cycle number, magnitude and frequency on the ratcheting and hence the structural response. These tests gave insight into the relationship between strain magnitude and ratcheting, the significance of high-frequency, low-magnitude daily cycles and the impact of increasing movements beyond the 40 mm limit in PD 6694-1:2011 (BSI, 2020). Thermal cycles were applied in displacement control since soil resistance is typically small compared with the restrained expansion force of a bridge deck (Card and Carder, 1993). The tests carried out are summarised in Table 3.

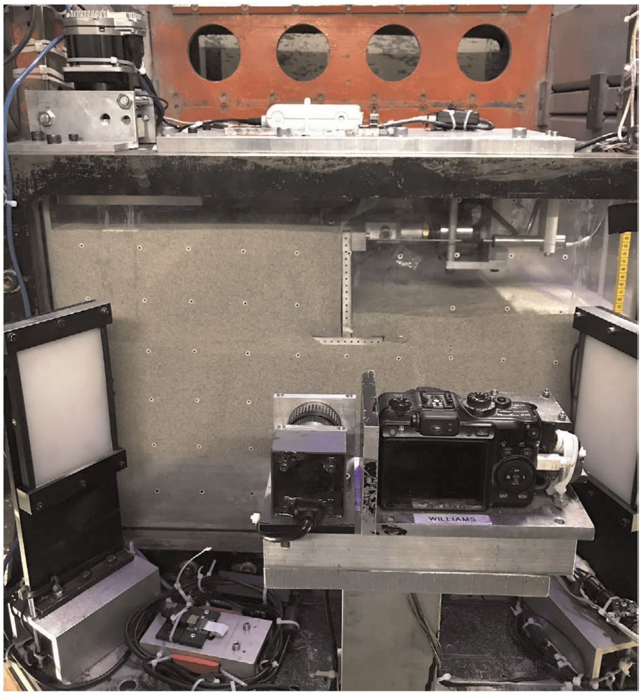

Figure 5. Assembled integral bridge model loaded onto centrifuge swing

Table 3. Centrifuge tests carried out

Test	Configuration
1	Reference configuration: stiff abutment, dense backfill and fixed abutment–foundation connection
2	Loose backfill
3	Pinned abutment–foundation connection
4	Reference configuration, double-amplitude movements
5	Flexible abutment, loose backfill
6	Flexible abutment, dense backfill
7	Reference configuration, geofoam inclusion
8	Reference configuration, small-amplitude daily cycles

4. Results

Results from the eight centrifuge tests are presented to demonstrate the suitability of the model in generating a ratcheting response and in responding to different parameters of influence. All the results were scaled to represent the behaviour of the full-size integral bridge.

4.1 Model performance

Figure 6 shows the applied displacements and corresponding bridge deck axial force recorded for a representative test, with equivalent stress provided on a secondary axis for a deck thickness of 1.5 m. Displacements were applied consistently around the ±20 mm target, with the variations observed considered to be no larger than those in a real deck due to annual temperature fluctuations. The increase in deck force over the cycles is a result of strain ratcheting occurring in the backfill material. This followed a decaying exponential trend, similar that found by Springman *et al.* (1996) and England *et al.* (2000). The soil settlement observed following displacement cycles is shown in Figure 7, with the profile resembling that discussed by Tatsuoka *et al.* (2009). This is indicative of the strain accumulation occurring over cycles, which caused the observed pressure ratcheting.

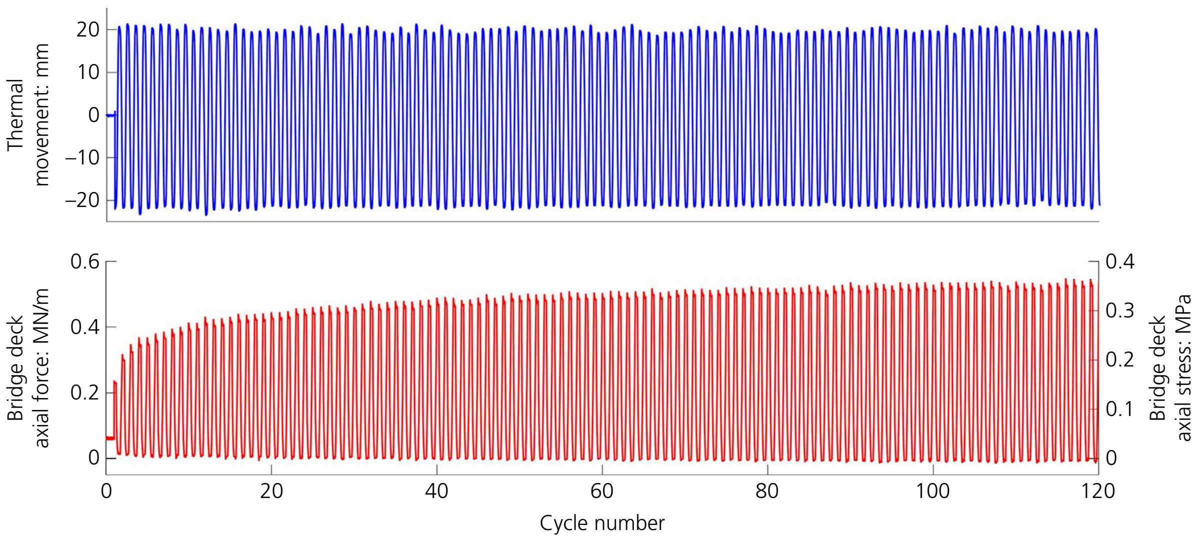

Figure 6. Applied thermal movements and corresponding response in deck force

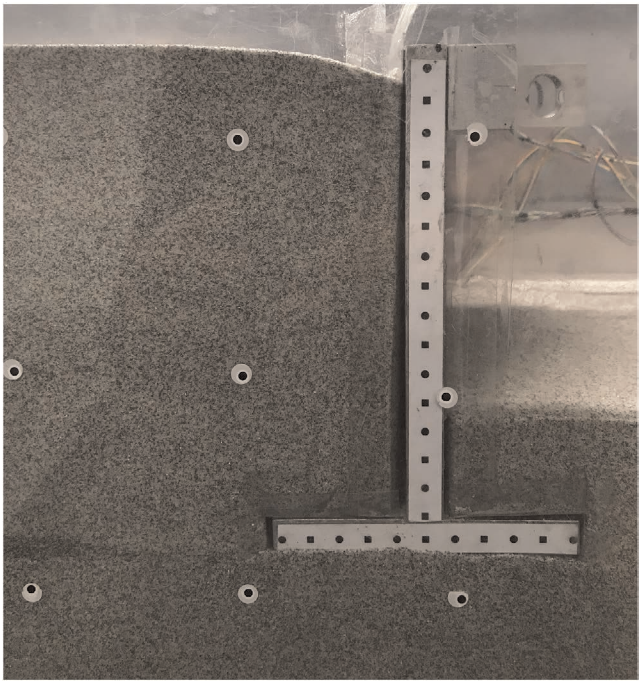

Figure 7. Soil settlement trough observed following thermal cycles

4.2 Actuation system control

Following the first three tests, control of the actuator was improved by introducing feedback from the LVDT into a C++ script; this increased the accuracy of displacement cycles, allowing a relatively constant displacement amplitude to be applied. Figure 8 compares the displacement and loading traces from an initial test without LVDT control and a subsequent test with a different soil–structure configuration. Both show a consistent cycling around the ±20 mm mark, but the control was clearly improved with LVDT input. The gradual reduction in applied displacements due to bending of the actuator frame, most notable towards the beginning as the ratcheting rate was high, was eliminated. Figure 8 shows how the corresponding increase in deck force became smoother with the improved control, although it was also stable enough without it.

4.3 Number, magnitude and frequency of thermal movements

Advanced control over the actuator allowed soil ratcheting to be examined in the context of applied strain magnitude, strain rate and hysteresis. Figure 9 shows three displacement traces applied during separate tests of the same soil–structure configuration. Trace A features an initial 120 cycles at ±20 mm magnitude, simulating seasonal movements through the design life at the limit defined by the LEM of PD 6694-1:2011 (BSI, 2020). An additional 600 cycles were then applied to observe the long-term progression of ratcheting. Following this, 20 cycles of double amplitude were introduced, followed by a series of even larger amplitude cycles. Finally, the initial ±20 mm movements were reapplied to explore the influence of strain history. Trace B was similar to trace A, except that applied displacements were doubled to emulate a larger bridge deck with an increased thermal response. Trace C commenced with small movements to observe the point at which ratcheting was initiated. Beyond this, the interaction of daily and seasonal cycles was investigated, as well as progressive cycle magnitudes.

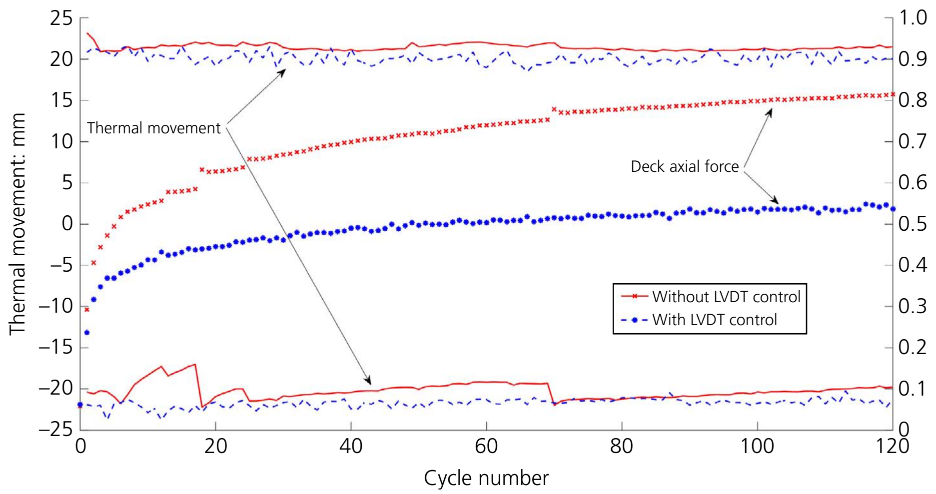

Figure 8. Comparison of applied movements and deck response after control improvements

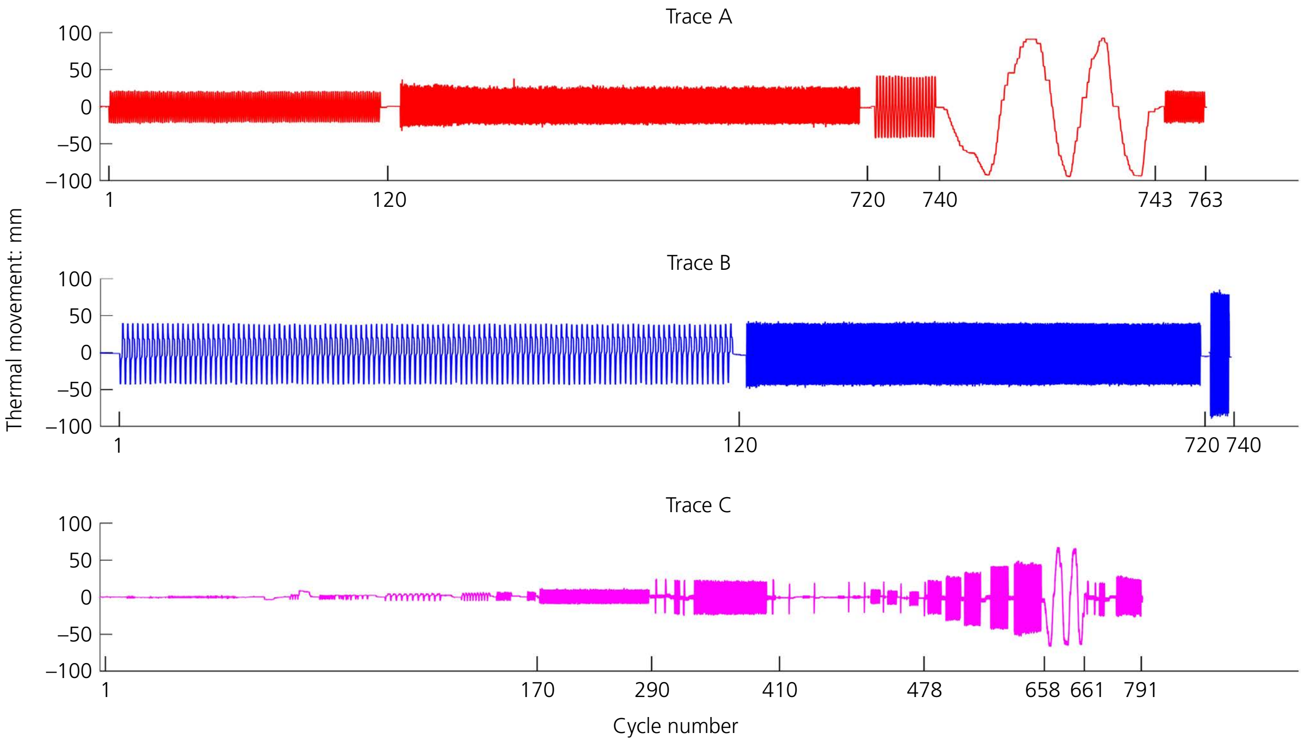

Figure 9. Applied thermal movement regimes for three separate tests

Figure 10 shows trace C from Figure 9 along with the corresponding bridge deck response. From this, it is possible to gain insight into several facets of the ratcheting mechanism, including:

- the threshold at which ratcheting begins
- long-term ratcheting trends
- the relationship between daily and seasonal cycles
- the impact of cycle magnitude on the rate of ratcheting

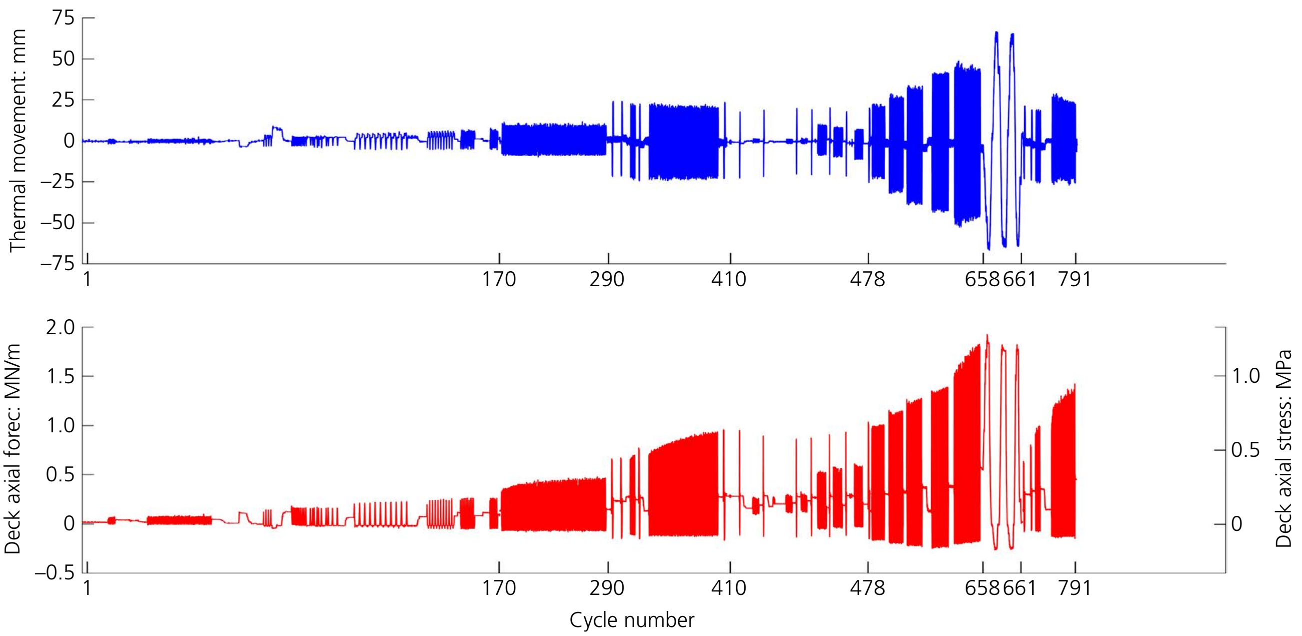

Figure 10. Thermal movements and deck force response for a complex cycle regime

- the influence of large-magnitude and low-frequency cycles
- the effect of strain history.

The large-magnitude cycles show the presence of creep, which lowered the force considerably in a short space of time. This demonstrates the rate dependence of the problem and hence the importance of choosing a suitably slow cycling rate despite it being a dry, cohesionless material – something not considered by Springman *et al.* (1994).

4.4 Abutment–footing connection

With three of the four experiments cited in PD 6694-1:2011 (BSI, 2020) modelling a pin-based abutment without a foundation (England *et al.*, 2000; Tan and Lehane, 2007; Tapper and Lehane, 2004), the influence of the abutment–foundation connection was investigated. Figure 11 shows the deflected shape of a fixed connection case as the abutment was pushed 20 mm into and away from the backfill. Global rotation of the abutment–foundation system was observed, accompanying the expected deflection. As well as releasing some of the foundation bending moments otherwise expected, this rotation reduced the abutment deflections required to remain compatible with the prescribed thermal movement. This resulted in a deflected shape somewhere between that of a perfectly fixed and pinned case, influencing the distribution of resistive earth pressures in the process. Additionally, the force required to cause the rotation, predominantly due to the compression of soil beneath the footing, affected the peak abutment bending moment alongside the ratcheting pressures. Asymmetry

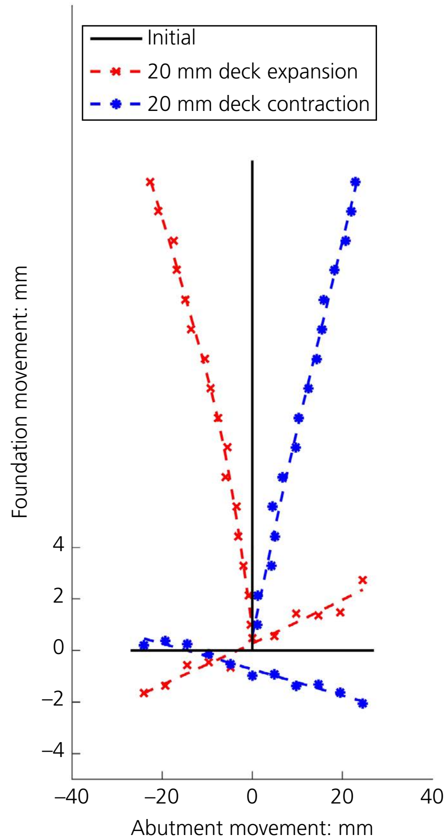

Figure 11. Deflected shape with abutment–foundation fixity

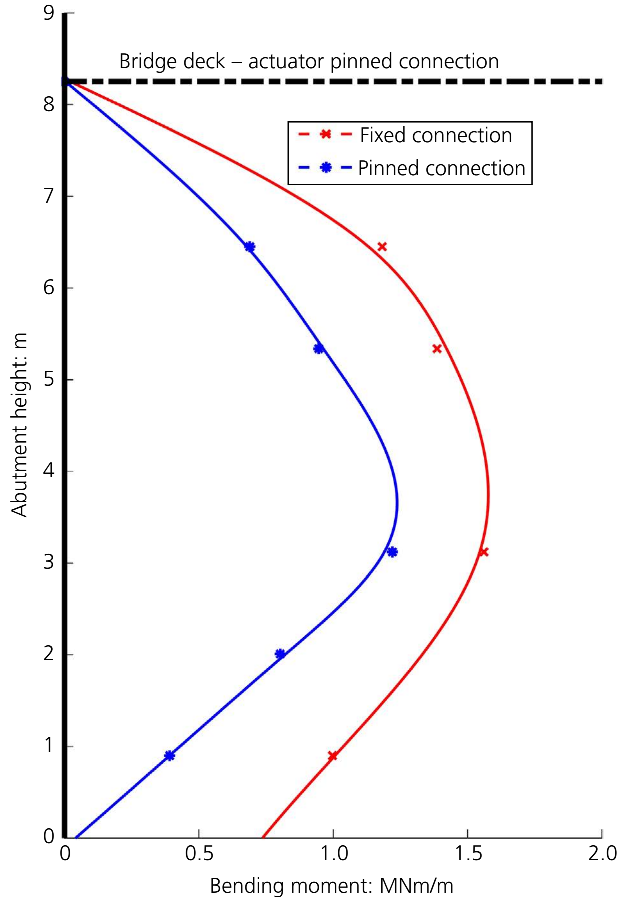

Figure 12. Bending moment comparison for fixed and pinned abutment–foundation connection

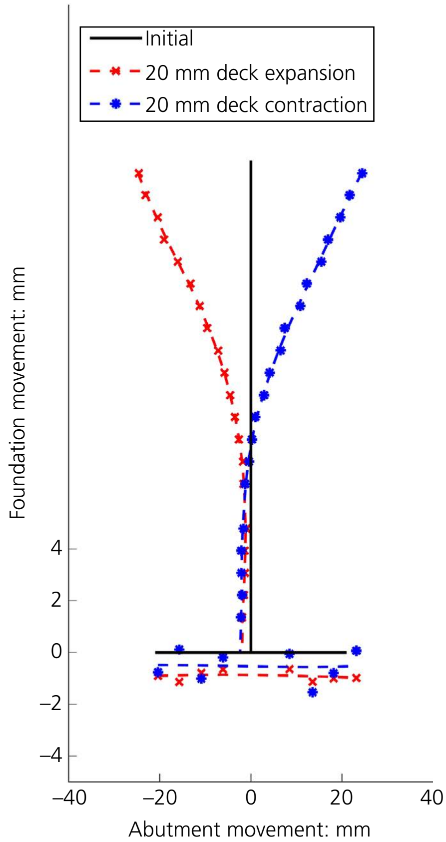

Figure 13. Deflected shape of fixed base, flexible abutment

of the response can also be seen through the off-centre rotation of the foundation during deck contraction.

The influence of foundation type on the abutment bending moment distribution is shown in Figure 12. As noted in Section 3.2.2, the two configurations were identical except for the replacement of the bolted abutment–foundation connection with a hinge. A 25% increase in peak bending moment occurred with the fixed connection compared with the pinned connection. This is because of the generation of restraining pressures beneath the foundation as it tried to rotate, in addition to those from compression of the backfill soil, thus requiring a larger bridge deck force to achieve the same magnitude of thermal movements. Moreover, since the abutment in the fixed case transferred its moment to the foundation, the lower half of the bending moment distribution was significantly higher.

4.5 Relative stiffness

Four tests were carried out to investigate the influence of relative soil–structure stiffness on the response of the integral bridge, combining either a stiff (1 m, $EI = 2.1 \times 10^6$ kN.m^2/m) or flexible (0.4 m, $EI = 1.4 \times 10^5$ kN.m^2/m) RC abutment with a dense ($I_\mathrm{d} = 85\%$) or loose ($I_\mathrm{d} = 40\%$) backfill soil.

The deflected shape of the flexible structure with dense backfill is shown in Figure 13, which can be compared with the stiff case response shown in Figure 11. Figure 13 shows that deflections were restrained until around one-third of the abutment height, much higher up than for the stiff abutment. This is because the flexible wall was unable to push the relatively stiff backfill at depth, thus having a major influence on the lateral earth pressures imposed on the abutment. While the foundation rotated when fixed to the stiff abutment, with the flexible structure, the foundation translated and settled instead. The low curvature towards the base of the abutment is indicative of the small bending moments transferred to the foundation compared with the stiffer abutment case. In this respect, the flexible abutment more closely resembled the behaviour expected from a pinned abutment–foundation connection.

Soil displacement vectors, found by tracking sand particles using PIV, for the four stiffness cases are presented in

Figure 14. These reflect the movement of soil from its initial position to its position at the end of testing, with the abutment returned to its original location. In all cases, soil ratcheting was characterised by a rotational mechanism extending backwards from the abutment, with variation in the degree of rotations depending on the relative stiffness. The depth of influence was roughly down to the mid-height of the abutment in all cases and there was limited soil movement surrounding the foundation. This presents a different perspective on the notion that particle rearrangement causes stress dissipation

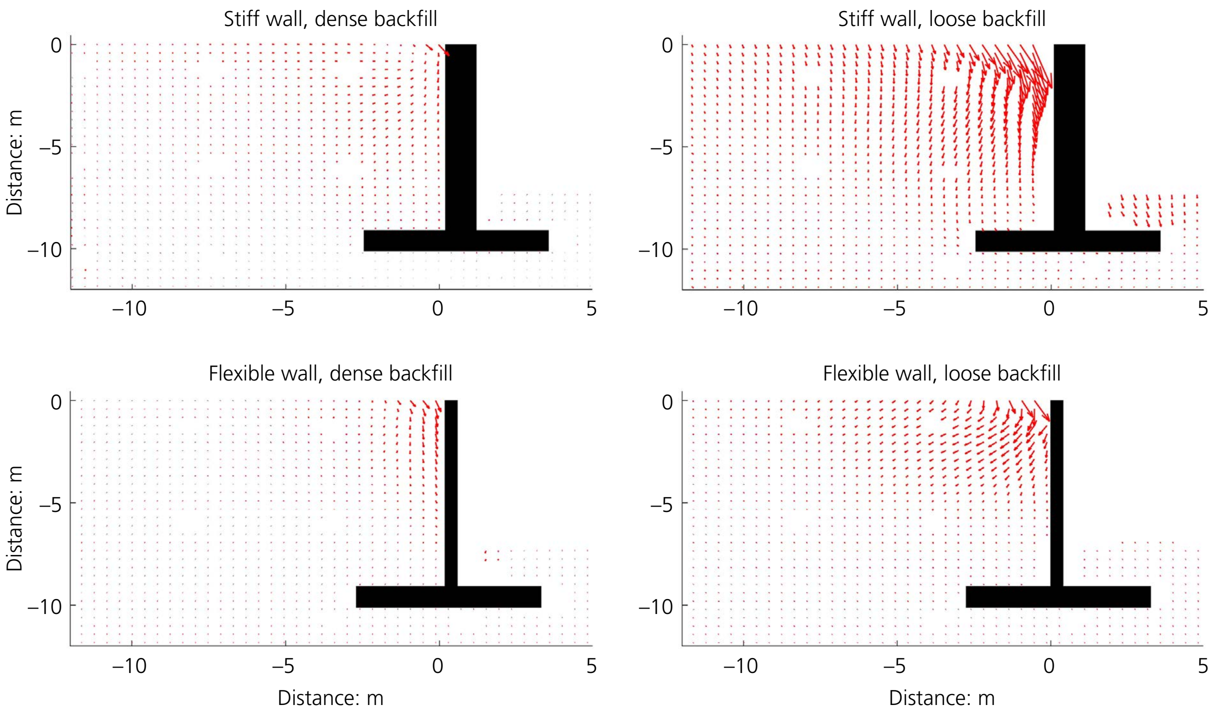

Figure 14. Soil displacement vectors over the test duration

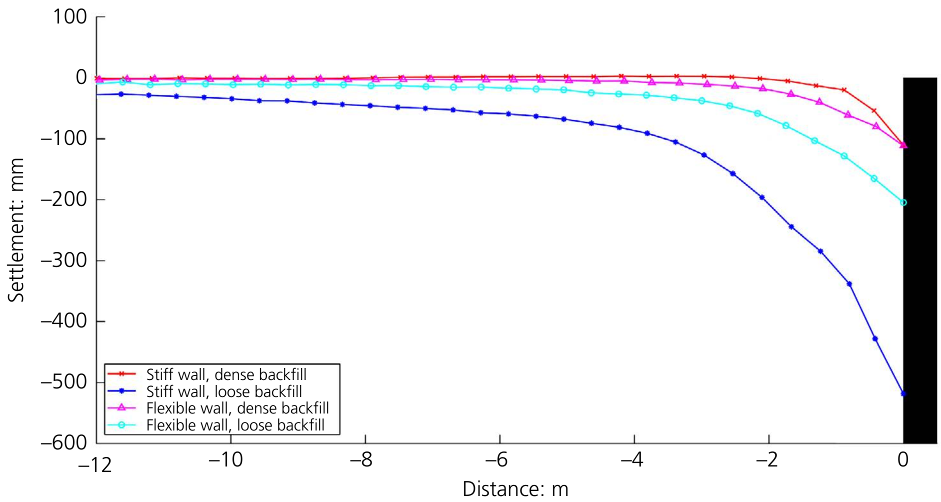

Figure 15. Soil settlement trough following thermal cycles

around the base for a model with no rigid bottom boundary, as discussed by Denton *et al*. (2011) and reflected in the constant, *C*, in the LEM in PD 6694-1:2011 (BSI, 2020) accounting for foundation soil stiffness.

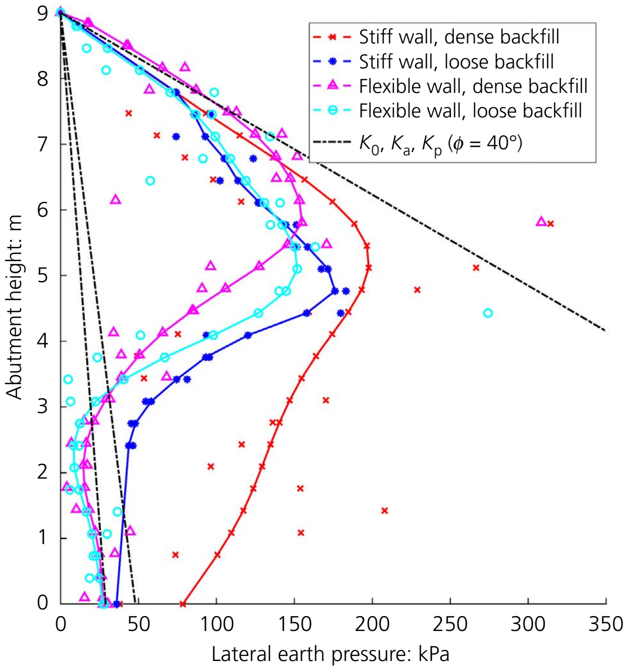

Figure 16. Lateral earth pressures acting on the abutment due to strain ratcheting of backfill; K_0, K_a and K_p = at-rest, active and passive earth pressure distributions respectively, and ϕ = friction angle

The mechanism shown through the vectors is linked to the extent of soil settlement during bridge deck contractions, which persisted once the abutment returned to its original position, as shown in Figure 15. The results show that the loose backfill settled considerably more than the dense case. The settlement observed in both dense tests appears to be largely unaffected by the abutment stiffness, while a greater volume change behind the stiff wall in the loose case caused the larger settlements. The settlement troughs in Figure 15 indicate the extent of periodic maintenance that may be required behind the abutment to maintain a smooth bridge approach during its design life, or alternatively, the length of an approach slab needed to span the gap. None of the tests found surface heave to occur in the far field, in contrast to the numerical work of Mitoulis *et al*. (2016).

The influence of relative soil–structure stiffness on earth pressures is shown in Figure 16. In all cases, the pressure peaks were above the mid-height of the abutment, agreeing with the numerical work of Sandberg *et al*. (2020) and Wiechecki *et al*. (2023) rather than the LEM in PD 6694-1:2011 (BSI, 2020). Pressure peaks in the flexible abutments occurred higher than in their stiff abutment counterparts, and dropped off sooner due to smaller deflections towards the foundation, which therefore resulted in lower net pressures. It is worth noting that the use of Hostun sand, with a lower friction angle than type 6N/P material, will likely have led to an underestimate of pressures according to PD 6694-1:2011 (BSI, 2020). These plots were used to chart the development of the lateral earth pressure coefficient (*K*) with cycle progression. As shown in Figure 17, all of the

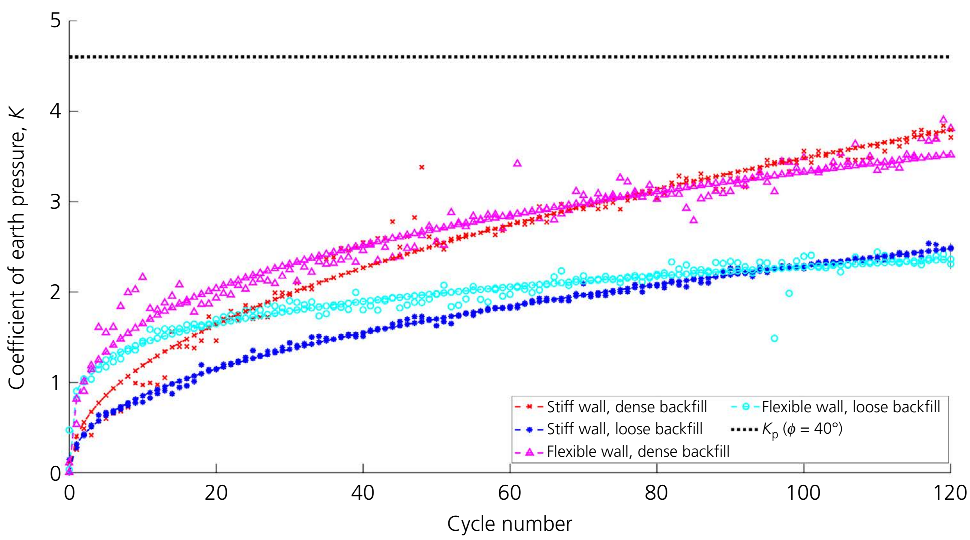

Figure 17. Development of lateral earth pressure coefficient over cycles

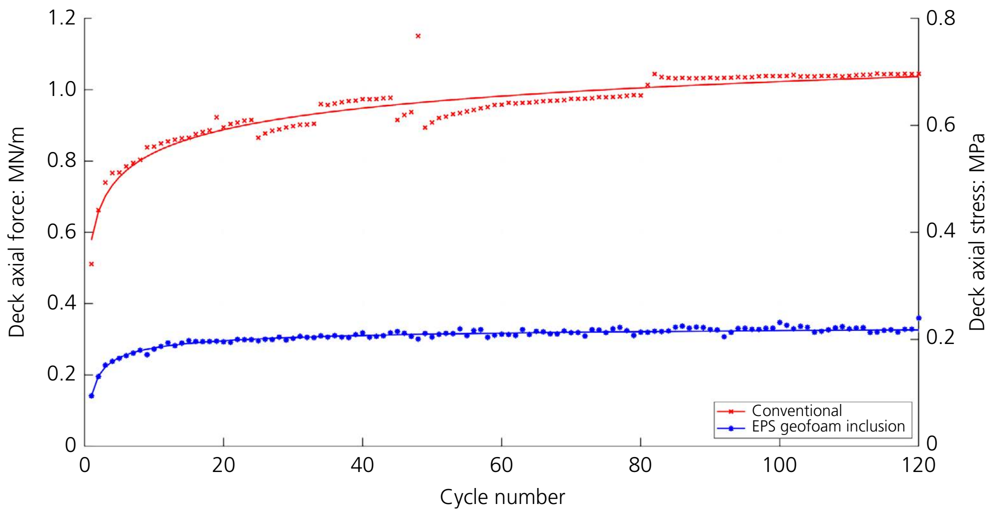

Figure 18. Mitigating effect of a compressible inclusion on earth pressure build-up

traces exhibited a decaying exponential trend, with the dense soils mobilising a considerably higher value than loose soils. This build-up occurred more rapidly and decayed more quickly with the flexible abutments as they interacted with a shallower depth of soil. Future work may look to calibrate numerical models using the data from Figures 16 and 17.

4.6 Mitigation measures

An EPS geofoam block, 1.2 m thick (20 mm at model scale), was placed between the abutment and backfill to investigate the impact of a compressible inclusion on bridge response. The results, presented in Figure 18, demonstrate that the geofoam effectively reduced the bridge deck force (a proxy for earth pressure) by 70% over the 120 cycles of ±20 mm movement. Additionally, the geofoam appeared to stabilise the ratcheting behaviour much earlier in the bridge's operational life. Figure 19 shows the configuration following testing. Addressing the concern of Carder and Card (1997), it appears that the material remained sufficiently elastic to prevent gaps and bulges, and it continued performing until the end of testing. The foam rebounded at the top of the abutment where soil settlement occurred, which is something a run-on slab could mitigate.

4.7 Varying abutment height

By increasing centrifugal acceleration, it was possible to scale the same model to different dimensions within the same test. Even if the soil had previously been disturbed, the higher stress state reached meant that the results were still valuable. At the end of the cycle regime shown in Figure 10, carried out at 60***g***, the model was taken to 100***g***,

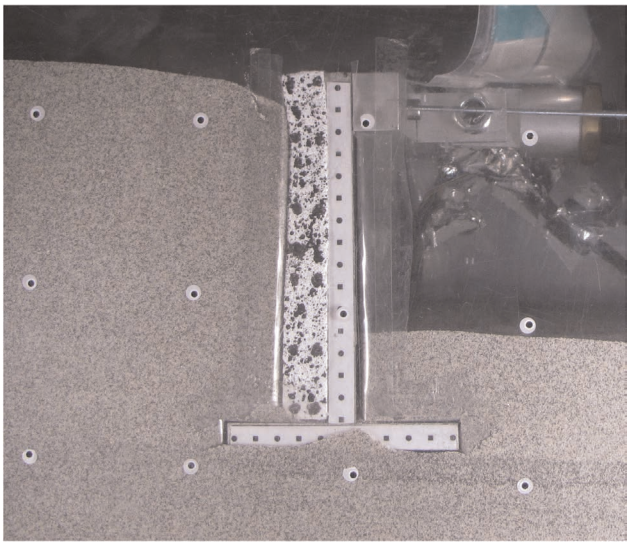

Figure 19. EPS geofoam following testing

scaling the abutment to 15 m from the original 9 m. This also scaled the *EI* of the abutment wall from 2.13×10^6 kN.m^2/m to 9.94×10^6 kN.m^2/m. The load cell traces from these tests are compared in Figure 20. For the 1.6 times increase in abutment height, the load required to push the abutment into the backfill tripled due to the greater volume of soil to strain and because this soil existed at a stiffer state due to the increased confinement. The ratcheting trends in both responses were similar, suggesting consistency across scales.

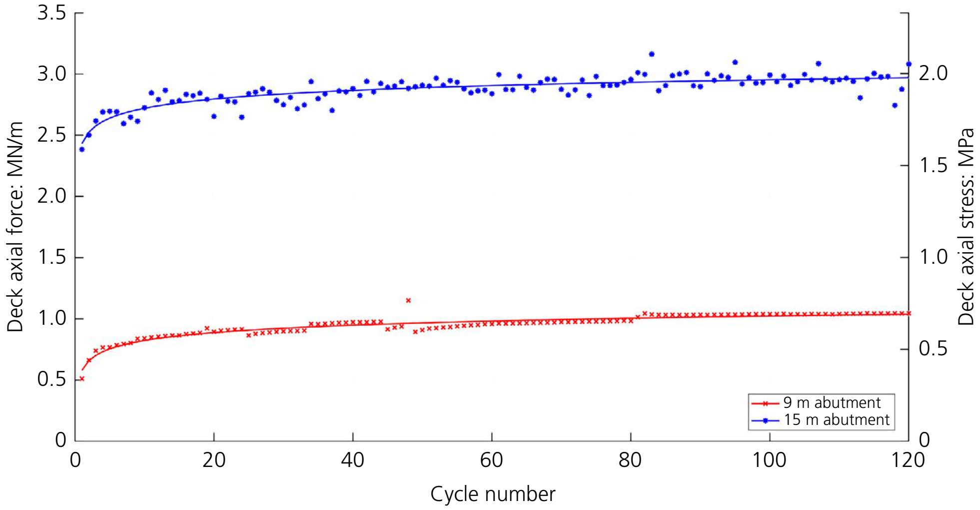

Figure 20. Comparison of force required to push a 9 m and 15 m abutment into backfill over thermal cycles

5. Conclusions

Uncertainty in the LEM of PD 6694-1:2011 (BSI, 2020) contributes to the conservative design of integral bridges, which are in some cases made unfeasible, thus driving designers to solutions that miss improvement opportunities presented by the interaction between the abutment and backfill soil. The most recent integral bridge research cited in PD 6694-1:2011 (BSI, 2020) was in 2008, over 15 years ago, hence further investigation is needed to drive design approaches forward.

This paper described a small-scale centrifuge model developed to investigate the ratcheting behind integral bridges, with the results from eight test configurations leading to the following conclusions:

(*a*) Geotechnical centrifuge modelling allows key parameters influencing the soil strain ratcheting mechanism associated with integral bridges to be tested at a realistic soil stress state, therefore offering an effective means to investigate and improve design code prescriptions.
(*b*) The rate and extent of ratcheting is dependent on the magnitude of thermal movements, with a threshold at which the pressure increase begins, which is not considered in the LEM of PD 6694-1:2011 (BSI, 2020). Also, notable soil stress relaxation with creep was observed when changing directions at high load, which modellers should be aware of.
(*c*) Global mechanisms such as foundation settlement, sliding and rotations of the spread footing were found to occur with thermal cycles, as also observed by Springman *et al*. (1996). These alter the abutment deflected shape, bending moment distribution and ratcheting pressures generated, yet are not accounted for in the LEM of PD 6694-1:2011 (BSI, 2020). Consideration of these could improve the efficiency of designs.
(*d*) The relative stiffness of the abutment and backfill was significant in altering the magnitude and distribution of earth pressures acting on the abutment following ratcheting. These are not accounted for in the K_d^* equation of the LEM in PD 6694-1:2011 (BSI, 2020), but future inclusion could allow practitioners to improve the performance of their designs.
(*e*) The peak lateral earth pressure following ratcheting occurred in the top half of the abutment, rather than at mid-height, in agreement with the work of Sandberg *et al*. (2020) and Wiechecki *et al*. (2023). This could be used to rationalise designs based on revised net pressure distributions in place of the LEM in PD 6694-1:2011 (BSI, 2020).
(*f*) Tracking soil movement throughout testing showed a rotational mechanism extending to a depth of around half the abutment height, with small soil movements around the foundation. This casts doubt over the extent of stress dissipation at the base of the abutment, and hence the parameter *C* in the K_d^* equation of the LEM in PD 6694-1:2011 (BSI, 2020).
(*g*) Use of geofoam as a compressible inclusion reduced the bridge deck axial force (a proxy for earth pressures generated) by 70%, and continued to perform over the design life of seasonal thermal cycles. Further physical modelling of different compressible inclusion thicknesses and materials should be carried out.

These findings suggest that geotechnical centrifuge testing, alongside the field instrumentation of long-span integral bridges, can generate the data required to inform future design codes that better reflect soil strain ratcheting behaviour. Moreover, they can help to justify the use of larger deck lengths similar to those already built overseas, maximising the benefits of integral bridge design and construction.

Acknowledgements

The authors would like to acknowledge National Highways and the EPSRC CDT in Future Infrastructure and Built Environment (FIBE2 CDT) for funding this project, as well as Gavin & Doherty Geosolutions (GDG) Ltd for their support.

REFERENCES

Abdel-Fattah MT, Abdel-Fattah TT and Hemada AA (2018) Nonlinear finite-element analysis of integral abutment bridges due to cyclic thermal changes. *Journal of Bridge Engineering* **23(2)**: article number 8, https://doi.org/10.1061/(asce)be.1943-5592.0001183.

Argyroudis S, Palaiochorinou A, Mitoulis S and Pitilakis D (2016) Use of rubberised backfills for improving the seismic response of integral abutment bridges. *Bulletin of Earthquake Engineering* **14**: 3573–3590.

Barker KJ and Carder DR (2000) *Performance of the Two Integral Bridges Forming the A62 Manchester Road Overbridge.* Transport Research Laboratory, Wokingham, UK, TRL Report 436..

Barker KJ and Carder DR (2001) *Performance of an Integral Bridge over the M1-A1 Link Road at Bramham Crossroads Agency.* Transport Research Laboratory, Wokingham, UK, TRL Report 521.

BSI (2020) PD 6694-1:2011+A1:2020: Recommendations for the design of structures subject to traffic loading to BS EN 1997-1:2004 +A1:2013. BSI, London, UK.

Card GB and Carder DR (1993) *A Literature Review of the Geotechnical Aspects of the Design of Integral Bridge Abutments.* Transport Research Laboratory, Wokingham, UK, TRL Report 52.

Carder DR (1998) *A Comparison of Embedded and Conventional Retaining Wall Design Using Eurocode 7 and Existing UK Design Methods.* Transport Research Laboratory, Wokingham, UK, TRL Report 320.

Carder DR and Card GB (1997) *Innovative Structural Backfills to Integral Bridge Abutments.* Transport Research Laboratory, Wokingham, UK, TRL Report 290.

Carder DR, Barker KJ and Darley P (2002a) *Suitability Testing of Materials to Absorb Lateral Stresses Behind Integral Bridge Abutments.* Transport Research Laboratory, Wokingham, UK, TRL Report 552.

Carder DR, Darley P and Bush DI (2002b) *Specification for Suitability Testing of Stress Absorbing Materials Behind Integral Bridge Abutments.* Transport Research Laboratory, Wokingham, UK, TRL Report 553.

Caristo A, Barnes J and Mitoulis SA (2018) Numerical modelling of integral abutment bridges under seasonal thermal cycles. *Proceedings of the Institution of Civil Engineers – Bridge Engineering* **171(3)**: 179–190, https://doi.org/10.1680/jbren.17.00025.

Clayton CRI, Xu M and Bloodworth A (2006) A laboratory study of the development of earth pressure behind integral bridge abutments. *Géotechnique* **56(8)**: 561–571, https://doi.org/10.1680/geot.2006.56.8.561.

Cosgrove EF and Lehane BM (2003) Cyclic loading of loose backfill placed adjacent to integral bridge abutments. *International Journal of Physical Modelling in Geotechnics* **3(3)**: 9–16, https://doi.org/10.1680/ijpmg.2003.030302.

Craig RF and Knappett J (2020) *Craig's Soil Mechanics*, 9th edn. CRC Press, Boca Raton, FL, USA.

Darley P and Alderman GH (1995) *Measurement of Thermal Cyclic Movements on Two Portal Frame Bridges on the M1.* Transport Research Laboratory, Wokingham, UK, TRL Report 165.

Darley P and Carder DR (1998) *Consultation Document on Suitability Tests for Stress Absorbing Layers Behind Integral Bridge Abutments.* Transport Research Laboratory, Wokingham, UK, TRL Report 328.

Darley P, Carder DR and Alderman GH (1996) *Seasonal Thermal Effects on the Shallow Abutment of an Integral Bridge in Glasgow.* Transport Research Laboratory, Wokingham, UK, TRL Report 178.

Darley P, Carder DR and Baker KJ (1998) *Seasonal Thermal Effects over Three Years on the Shallow Abutment of an Integral Bridge in Glasgow.* Transport Research Laboratory, Wokingham, UK, TRL Report 344.

Denton S, Riches O, Christie T and Kidd A (2011) *Developments in integral bridge design*. In *Bridge Design to Eurocodes: UK Implementation* (Denton S (ed.). ICE Publishing, London, UK, pp. 463–480.

England GL, Tsang NCM and Bush DI (2000) *Integral Bridges – A Fundamental Approach to the Time-Temperature Loading Problem*. Crown Copyright and Thomas Telford Limited, London, UK.

HA (Highways Agency) (2003) *DMRB, Volume 1, Section 3, Part 12, BA 42/96: Highway structures: Approval procedures and general design. General design. Design of integral bridges (includes Amendment No. 1 dated May 2003), HA, London, UK.*

Hambly EC (1997) Integral bridges. *Proceedings of the Institution of Civil Engineers – Transport* **123(1)**: 30–38, https://doi.org/10.1680/itran.1997.29177.

Khodair YA and Hassiotis S (2005) Analysis of soil-pile interaction in integral abutment. *Computers and Geotechnics* **32(3)**: 201–209, https://doi.org/10.1016/j.compgeo.2005.01.005.

Kim DS, Kim NR, Choo YW and Cho GC (2013) A newly developed state-of-the-art geotechnical centrifuge in Korea. *KSCE Journal of Civil Engineering* **17(1)**: 77–84, https://doi.org/10.1007/s12205-013-1350-5.

Kolay C, Prashant A and Jain SK (2013) Nonlinear dynamic analysis and seismic coefficient for abutments and retaining walls. *Earthquake Spectra* **29(2)**: 427–451, https://doi.org/10.1193/1.4000141.

Lancellotta R (2009) *Geotechnical Engineering*, 2nd edn. CRC Press, London, UK.

Lehane BM, Keogh DL and O'Brien EJ (1999) Simplified elastic model for restraining effects of backfill soil on integral bridges. *Computers and Structures* **73(1–5)**: 303–313, https://doi.org/10.1016/S0045-7949(98)00247-8.

Madabhushi G (2014) *Centrifuge Modelling for Civil Engineers.* CRC Press, London, UK.

Mitoulis SA, Palaiochorinou A, Georgiadis I and Argyroudis S (2016) Extending the application of integral frame abutment bridges in earthquake-prone areas by using novel isolators of recycled materials. *Earthquake Engineering & Structural Dynamics* **45(14)**: 2283–2301.

Morley DG, Madabhushi GSP, Thusyanthan I and Shires R (2022) Modelling of an integral bridge abutment under cyclic thermal loading. In *Proceedings of the 10th International Conference on Physical Modelling in Geotechnics (ICPMG), Daejeon, Korea* (Chung M, Kim SR, Kim NR *et al.* (eds)). International Society for Soil Mechanics and Geotechnical Engineering (ISSMGE), London, UK, pp. 388–391.

Morley DG, Asia YB, Madabhushi GSP, Thusyanthan I and Sakufiwa D (2024) Influence of relative stiffness on integral bridge design. In *Climate Change Adaptation from Geotechnical Perspectives. CREST 2023*. (Hazarika H, Haigh SK, Chaudhary B, Murai M and Manandhar S (eds)). Lecture Notes in Civil Engineering, 1st edn, Springer, Singapore, vol. 447.

Ng C, Springman S and Norrish A (1998) Soil-structure interaction of spread-base integral bridge abutments. *Soils and Foundations* **38(1)**: 145–162.

Sandberg J, Magnino L, Nowak P, Wiechecki M and Thusyanthan I (2020) The integral bridge design concept for the third runway at Heathrow, UK. *Proceedings of the Institution of Civil Engineers – Bridge Engineering* **173(2)**: 112–120, https://doi.org/10.1680/jbren.19.00044.

Schofield AN (1980) Cambridge geotechnical centrifuge operations. *Géotechnique* **30(3)**: 227–268, https://doi.org/10.1680/geot.1980.30.3.227.

Skorpen SA, Kearsley EP and Kruger EJ (2018) Measured temperature and shrinkage effects on a 90 m long integral bridge in South Africa. *Proceedings of the Institution of Civil Engineers – Bridge Engineering* **171(3)**: 169–178, https://doi.org/10.1680/jbren.17.00019.

Skorpen SA, Kearsley EP, Clayton CRI and Kruger EJ (2020) Structural monitoring of an integral bridge in South Africa. *Proceedings of the Institution of Civil Engineers – Smart Infrastructure and Construction* **173(3)**: 63–72, https://doi.org/10.1680/jsmic.20.00001.

Springman S, Norrish A and Wilkinson K (1994) A device for cyclic displacement-controlled actuation of an integral bridge abutment. In *Centrifuge* (Leung C, Lee F and Tan T (eds)). Balkema, Rotterdam, the Netherlands, vol. 94, pp. 163–168.

Springman SM, Norrish ARM and Ng CWW (1996) *Cyclic Loading of Sand Behind Integral Bridge Abutments*. Transport Research Laboratory, Wokingham, UK, TRL Report 146.

Stanier SA, Blaber J, Take WA and White DJ (2016) Improved image-based deformation measurement for geotechnical applications. *Canadian Geotechnical Journal* **53(5)**: 727–739.

Tan EL and Lehane BM (2007) *Lateral Stress Development on Integral Bridge Abutments*. PhD thesis, University of Western Australia, Perth, Australia.

Tapper L and Lehane B (2004) Lateral stress development on integral bridge abutments. In *Proceedings of Australasian Conference on the Mechanics of Structures and Materials* (Deeks AJ and Hao H (eds)). CRC Press, Perth, Australia, vol. 2, pp. 1069–1075.

Tatsuoka F, Hirakawa D, Nojiri M *et al.* (2009) A new type of integral bridge comprising geosynthetic-reinforced soil walls. *Geosynthetics International* **16(4)**: 301–326, https://doi.org/10.1680/gein.2009.16.4.301.

Trenter NA (2004) Approaches to the design of cantilever retaining walls. *Proceedings of the Institution of Civil Engineers – Geotechnical Engineering* **157(1)**: 27–35, https://doi.org/10.1680/geng.2004.157.1.27.

UWA and QUC (University of Western Australia and Queens' University Canada) (2015) *GeoPIV-RG*. See http://www.geopivrg.com/ (accessed 14/05/2024).

White H (2007) *Integral Abutment Bridges: Comparison of Current Practice between European Countries and the United States of America*. Transportation Research and Development Bureau. Albany, NY, USA, Special Report 152.

Wiechecki M, Thusyanthan I, Nowak P and Sandberg J (2023) Soil–structure interaction behind integral bridge abutments. *Proceedings of the Institution of Civil Engineers – Geotechnical Engineering*, https://doi.org/10.1680/jgeen.22.00115 (in press).

Wood DM (2004) *Geotechnical Modelling*. Spon Press, Abingdon, UK.